A fracture-mechanics-based non-local damage model for crack prediction in brittle materials

Zhang Xiao-Bing[1], Li Jia[2*]

[1]LAMI, Université Blaise Pascal de Clermont, Montluçon, France;

[2]LSPM, CNRS UPR 3407, Université Paris XIII, Villetaneuse, France;

* Corresponding author: jia.li@univ-paris13.fr

Abstract: Description of crack initiation and crack growth is a principal aim of numerical simulations in fracture mechanics. In this work, we have established a non-local damage model based on the fracture mechanics for brittle materials. This non-local model associates the classical failure criteria for non-cracked materials and the Griffith criterion for cracked materials throughout a non-local approach. Consequently, this model can be used to predict the crack initiation as well as the crack growth. The maximal principal stress criterion was considered in the proposed non-local framework. It was shown that after the non-local treatment, the classical failure criteria can be used in the prediction of crack initiation and crack growth with different failure mechanisms. By using the proposed model, we carried out several numerical simulations on different specimens in order to assess the fracture process in brittle materials. From these studies, we can conclude that the present model can be used to deal with crack initiation and crack growth in brittle materials with high accuracy and efficiency.

Keywords: fracture, crack, damage, non-local model

1. Introduction

The fracture prediction of structures made of brittle materials is an important issue in engineering designs. In real structures, the failures are often initiated from a few geometrical weaknesses near which stress concentrations are formed. The stress concentrations are of many types and different levels. The failure prediction for all these stress concentrations is an essential research topic for scientists and engineers. However, it seems that fractures can be accurately predicted only for few types of stress states as so far. For brittle materials, failure criteria for two simple situations are commonly accepted:

1: Under uniform uniaxial tension, fracture occurs when the maximum tensile stress reaches the ultimate stress of the material:

$$\sigma \geq \sigma_c \tag{1}$$

2: For solids including a macrocrack, the crack grows when the Griffith criterion is fulfilled:

$$G \geq G_c \tag{2}$$

where G and G_c are respectively the energy release rate and its critical fracture value.

Unfortunately, these criteria have to be used separately: one for damage initiation and another for crack growth. In the cases when the stress distribution is not uniform but does not present a crack singularity, these criteria are no longer sufficient to describe accurate fracture conditions. Many factors such like stress gradient, multi-axial stress state or structure size may influence the material strength. With the aim of unifying these criteria in a single damage model and extending them to

more general cases, numerous fracture and damage models were proposed in the literature.

When the stress concentration presents a singularity weaker than the crack one, such a singularity can be found in the cases of sharp notches, interface cracking or cracks in ductile materials, criteria based on finite fracture mechanics were developed and reported in the literature. In simple words, these criteria are kinds of combinations of (1) and (2). [1-5]. Another class of fracture criteria was issued from the so-called cohesive models [6-10]. In all these criteria and models, one can distinguish a length scale parameter, such as the critical distance from the crack tip in finite fracture mechanics or the maximum separation distance in cohesive models.

The finite fracture concept can also be found in damage analyses. A wide variety of damage models have been proposed on the basis of continuum damage mechanics by introducing a length parameter [11-15]. The nonlocal models in a continuum damage setting, the gradient theory based damage models, the damage gradient models are some of the principal advances in this direction.

In this work, we have constructed a damage model by associating the maximal stress criterion with a non-local formalism. Moreover, equivalence has been illustrated between this non-local model and the Griffith-Irwin fracture criterion for crack propagation. Using the established non-local damage model, we carried out detailed numerical simulations on different specimens in order to study the efficiency and accuracy of the present approach. The numerical results show that the proposed damage model is capable to simulate the crack initiation as well as the crack growth in brittle composites with highly realistic description.

2: Non-local damage model

Numerous continuous damage models exist in the literature. In this work, we will use a simple failure criterion for brittle materials, i.e. the instantaneous damage model on the basis of the maximum stress criterion, namely:

$$D=\begin{cases}0 & \sigma_1<\sigma_c\\ 1 & \sigma_1\geq\sigma_c\end{cases} \qquad (3)$$

where σ_1 is the maximal principal stress and σ_c is the ultimate tensile stress of the material. It is clear that other more elaborate damage evolution laws exist and may be more efficient and physically more realistic for this class of materials. In the present work, (3) is adopted for simplicity.

Even though this strength criterion is commonly used in failure assessment of a non-cracked structure, however, it is not suitable to describe fracture due to cracks because of the stress singularity near the crack tips. In order to overcome this shortcoming, various methods have been proposed. Among these, the so-called non-local approaches are widely used. The basic idea of this approach consists in replacing the local damage driving force, i.e. σ_1 in the present case, by its

weighted average over a representative volume V [11]:

$$\tilde{\sigma}_1(\mathbf{x}) = \frac{1}{\int_V \alpha(\mathbf{x}-\mathbf{y})d\mathbf{y}} \int_V \alpha(\mathbf{x}-\mathbf{y})\sigma_1(\mathbf{y})d\mathbf{y} \tag{4}$$

In Equation (4), α(**x**- **y**) is a space weighting function which describes the mutual non-local interactions and depends only on the distance between the source point **x** and the receiver point **y**. By simplicity, we write:

$$\alpha(r) = \begin{cases} 0 & r > R \\ 1 - \dfrac{r}{R} & r \le R \end{cases} \tag{5}$$

where $r = \|\mathbf{x}-\mathbf{y}\|$; R is the radius of non-local action which defines the size of interaction zone for failure processes.

By means of the non-local principal stress, the damage model (3) can be rewritten as follows:

$$D = \begin{cases} 0 & \tilde{\sigma}_1 < \sigma_c \\ 1 & \tilde{\sigma}_1 \ge \sigma_c \end{cases} \tag{6}$$

3: Connection to the Griffith-Irwin criterion

In this section, we will prove that the non-local damage model (6) can be connected to the Griffith-Irwin criterion and therefore, can be used to predict crack growth. Consider a mode-I loaded macro-crack. According to the Williams asymptotic solution [16], the near-tip first principal stress is modulated by the stress intensity factor K_I as follows:

$$\sigma_1(r,\theta) = \frac{K_I}{\sqrt{2\pi r}}\left(1+\cos\frac{\theta}{2}\right)\left|\sin\frac{\theta}{2}\right| \tag{7}$$

Due to the symmetry, the maximal non-local principal stress is located at a point on the crack axis near the crack tip: $r = r_0, \theta = 0$. Therefore, from (4), (5), and (7):

$$\tilde{\sigma}_1(r_0) = \max_{r_0} \int_0^R \int_{-\pi}^{\pi} \frac{3}{\pi R^2}\left(1-\frac{r'}{R}\right)\frac{K_I}{\sqrt{2\pi r}}\left(1+\cos\frac{\theta}{2}\right)\left|\sin\frac{\theta}{2}\right| r' dr' d\theta' = 0 \tag{8}$$

On the one hand, if we assume that $\tilde{\sigma}_1(r_0)$ is the maximal value of $\tilde{\sigma}_1(r,\theta)$ near the crack tip, the element at the crack-tip is damaged when $\tilde{\sigma}_1(r_0) = \sigma_c$ according to the damage criterion (6). On the other hand, from the Griffith criterion of fracture, the crack grows when the energy release rate G attains its critical value G_c. For mode-I cracks, this criterion is equivalent to the Irwin criterion $K_I \ge K_{Ic}$, where K_{Ic} is the critical stress intensity factor. Therefore, the parameters R and r_0

can be found by resolving the following equation:

$$f(R) = \sigma_c - \max_{r_0} \int_0^R \int_{-\pi}^{\pi} \frac{3}{\pi R^2}\left(1-\frac{r'}{R}\right)\frac{K_{Ic}}{\sqrt{2\pi r}}\left(1+\cos\frac{\theta}{2}\right)\left|\sin\frac{\theta}{2}\right| r' dr' d\theta' = 0 \qquad (9)$$

with

$$r = \sqrt{\left(r_0 + r'\cos\theta'\right)^2 + \left(r'\sin\theta'\right)^2} \quad \tan\theta = \frac{r'\sin\theta'}{r_0 + r'\cos\theta'}$$

By using the non-local scheme (4) and with R calculated from Equation (9), the damage model (6) can directly be used to predict the crack growth. To this end, we just need to find the point (r_0, θ_0) near the crack tip where the non-local principal stress is maximal: when the non-local stress attaints the material strength, the crack grows to the point (r_0, θ_0) according to the Griffith-Irwin criterion.

The above-mentioned damage model was implemented into a Fast Fourier Transfer (FFT) code. The iterative method on the basis of FFT was originally proposed by for homogenizing linear and nonlinear composites [17]. The FFT-based formulation for a periodic heterogeneous cell with damage was developed according to the original FFT scheme [18]. Since an element in a structure is linearly elastic before its complete damage, the method of crack propagation evaluation used in this work is very similar to that adopted in linear fracture mechanics: An elastic calculation is first carried out for a cracked structure, and then crack progression and the corresponding remote load are determined according to the damage criterion (6). This procedure is then repeated after each small crack progression in the structure

4: Numerical examples and discussion

In this section, we will carry out a series of numerical calculations in order to assess the performance of the present fracture model in predicting the crack evolution in brittle and quasi-brittle materials. First, we will verify its accuracy in predicting crack growth with a cell containing a central crack under pure mode-I loading. Then cells with more complicated microstructure will be considered in order to evaluate its efficiency and potentiality.

4.1: Cells with a central crack

The first numerical example is a plane stress plate containing a central crack. In the numerical simulations, the dimension of the plate is $2h \times 2h = 10 \times 10\text{mm}^2$ with a central crack of different sizes, namely a = 0, 0.1, 0.3, 0.5, 1, 2, 3 and 4mm, here a = 0 represents a non-cracked plate. The stress intensity factors of such cracks can be found in any handbook of stress intensity factors. The mechanical properties of the material are: Young's modulus E = 3000 MPa, Poisson's ratio ν = 0.3, the ultimate stress σ_c = 72MPa, the critical stress intensity factor $K_{Ic} = 36\text{MPa}\sqrt{\text{mm}}$, the non-local action radius R=0.105mm and the radius of the damaged zone r_d=0.05mm. In order to investigate

the influence of the resolution finesse on the numerical results, the cell was discretized using different grids of regularly spaced Fourier points. The resolutions used for discretization are 100×100, 200×200, 400×400 and 600×600 pixels. The pure mode-I load is prescribed by imposing an average strain $\overline{\mathbf{E}} = \left\{\overline{E}_{11} \quad \overline{E}_{22} \quad \overline{E}_{12}\right\} = \overline{E}_{11}\left\{1 \quad -0.3 \quad 0\right\}$.

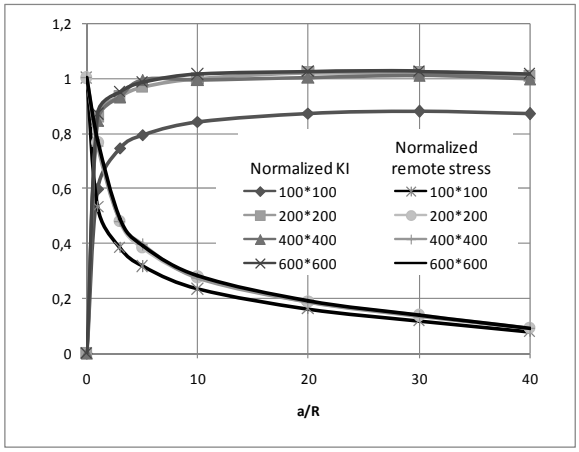

Figure 1: Normalized stress intensity factor K_I/K_{Ic} and normalized remote stresses σ^∞/σ_c as function of normalized semi-crack length a/R for mode-I loaded cracks at fracture

We first calculated the remote tensile loads σ^∞ for crack growth according to the damage criterion (7). The calculations were carried out for different crack length and with different discretization resolutions. The results of these calculations are reported in Figure 1. In this figure, the stress intensity factors are normalized by the critical value K_{Ic} ; the remote stresses are normalized by the ultimate stress σ_c of the material and the crack length is normalized by the non-local action radius *R*. From this figure, several remarks can be made:

1. When the crack is sufficiently long with respect to the non-local radius *R* ($a > 3R$), the stress intensity factors evaluated from the present non-local damage model for crack growth equal correctly the critical stress intensity factor of the material. This result confirms that the proposed damage model is equivalent to the criterion $K_I \geq K_{Ic}$ for mode-I cracks;
2. When the FFT discretization is sufficiently fine, the proposed damage model is independent of the FFT grid resolution.
3. The remote stress at fracture tends to the ultimate stress of material as the crack length tends to zero. In this case, the proposed crack growth criterion degenerates to the maximum stress criterion for non-singular stresses.

4.2: Cracking in concrete

The second example deals with a recurrent problem in concrete mechanics. The concrete is often modeled by a 3-phase particle composite where stiff and strong aggregate particles are embedded in a weaker and softer cement matrix. A third phase exists between these two phases, namely a thin

zone enveloping the aggregate particles. This thin zone of extremely weak material is the interfacial transition zone (ITZ). In the composite either the ITZ phase or the matrix phase may percolate. In the literature, the fracture of such a system is usually studied by means of lattice models constructed of bar or beam network [19-21].

In this example, a basic cell of 90×90mm² was discretized by a 600×600 FTT grid. The circular particles of diameters varying from 2 to 12mm were arbitrarily distributed in the cell. The thickness of the ITZ was chosen as 0.3mm. This thickness includes at least 2 pixels with the used grid. The density of the particles and ITZ attains 20% in volume. Following material constants were used in the simulations: $\sigma_c^{(matrix)} = 10\text{MPa}$; $\sigma_c^{(ITZ)} = 5\text{MPa}$; $\sigma_c^{(particle)} = \infty$ for ultimate stresses; $E^{(matrix)} = 20000\text{MPa}$; $E^{(ITZ)} = 30000\text{MPa}$; $E^{(particle)} = 40000\text{MPa}$ for Young's moduli and $K_{Ic}^{(matrix)} = 20\text{MPa}\sqrt{mm}$, $K_{Ic}^{(ITZ)} = 10\text{MPa}\sqrt{mm}$ and $K_{Ic}^{(particle)} = \infty$ for critical stress intensity factors. A traction load $\overline{\mathbf{E}} = \overline{E}_{11}\{1 \quad -0.3 \quad 0\}$ is prescribed on the cell. By resolving Equation (9), we obtained the non-local action radius R=1.5mm. The radius of the damaged spot is taken as r_d=0.5mm. As this spot can cover both matrix and ITZ, in practice, we take precautions such that the broken zone contains only points in the matrix or only points in the ITZ according to the location of the maximal non-local principal stress.

The results of the numerical simulations are presented in Figures 2. Figure 2a shows a basic cell with matrix in gray, particles in black and ITZ in white. Global response on average stress-strain is plotted in Figure 2d. Here the average stresses are normalized by the ultimate stress of the matrix. The average stress-strain curve of the cell clearly shows a quasi-brittle behavior that is inherent to concrete. The crack growth pattern at load peak is illustrated in Figure 2b. From this figure, we can observe that the pre-peak micro-cracking essentially occurs in the ITZ, which are the weakest phase confined to the outer rim of the stiff aggregates. This damage stage constitutes the entire hardening phase of the global response. After the peak, the cracks enter into the matrix. The crack growth pattern at the end of load is shown in Figure 2c. At this stage, the bridging between different damaged ITZs leads to rapid stiffness decrease of the cell. These results agree with those obtained in the literature using lattice analysis [19-21].

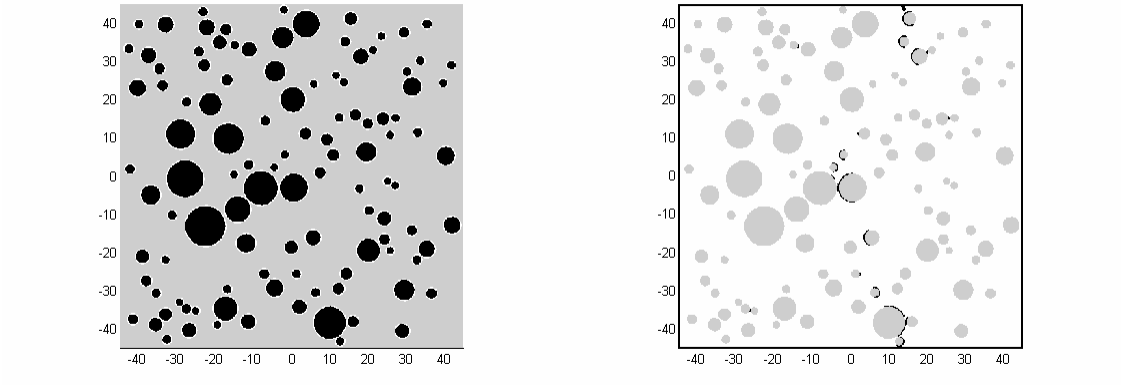

(a) (b)

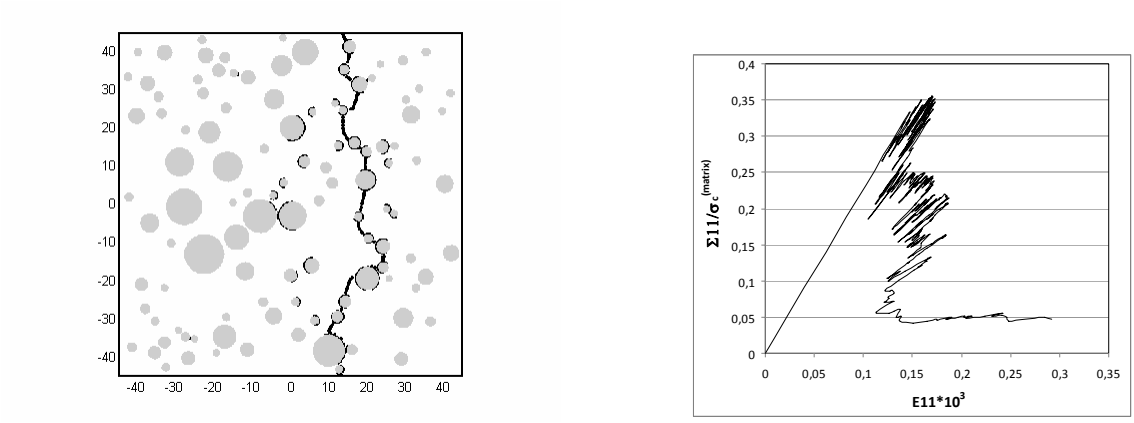

(c) (d)

Figure 2: Concrete plate containing unbreakable particles enveloped by ITZ (a), crack patterns at peak of the loading (b), at the end of the loading and global response (d) of the concrete plate

4.3: Fracture in laminate composites

Let's consider a plane strain composite laminate cell of dimension 20×18.2 mm² formed by 3 phases: matrix, fibres and interfaces. The thicknesses of these layers are: 0.625mm for matrix, 0.625mm for fibres and 0.025mm for interphases. The entire cell was divided into pixels by a 400×728 Fourier grid. Each layer of the composite is assumed to be linearly elastic and isotropic. The material parameters of each component are listed in Table 1:

Table 1: Material constants of the components

	E (MPa)	ν	σ_c (MPa)	K_{Ic} (MPa√mm)	R (mm)
Matrix (epoxy)	5100	0.35	100	50 or 200	0.105 or 1.486
Fibre (carbon)	210000	0.27	1400	700	0.105
Interphase	10451	0.3483	40 or 60	20 or 30	0.2906

The external loads can be applied by imposing average stresses $\Sigma_{11} > 0$, $\Sigma_{22} = \Sigma_{12} = 0$ or average strains $E_{11} > 0$, $E_{22} = E_{12} = 0$. The FFT simulations were carried out step by step with small crack growth (about 0.1mm) at each step until the full failure of the cell. We present hereafter a FFT simulation with a reference configuration, i.e., the basic cell subjected to a uniaxial tension by imposing average stresses $\Sigma_{11} > 0$ and $\Sigma_{22} = \Sigma_{12} = 0$ as remote loads.

Figure 3a illustrates the global response, i.e., the E_{11}–Σ_{11} curve of the cell during the loading. Figures 3b, shows the fracture patterns of the cell at the end of the failure process. With the aid of these figures, we can describe the fracture process of the composite as follows:

1. Under uniaxial tension, the global response of the composite laminate presents a saw-tooth snap-back feature. Each tooth represents the crack growth though a fibre layer;

2. When a short crack grows in a layer of matrix and meets a fibre, a high level load is needed to overcome this energy barrier. It first deviates a little into the interface or in the matrix before entering in the fibre;
3. When the crack grows in a layer of fibre and meets the matrix, it deviates slightly in the matrix before penetrating into the matrix. As the matrix strength is much lower than that of the fibre, the remote load drops significantly;
4. As the transversal main crack grows and becomes longer, the length of its deviations into the interfaces increases when it meets a fibre;
5. We can remark that the interface debonding acts as a crack arrestor as described in previous studies [3]. When the crack propagates in an interface, the crack tip mode mixity varies from mode I toward mode II. Its growth requires more and more energy according to the interface fracture criterion (Equation 15);

As a result of the interface debonding, the final fracture surfaces take a stair form as observed in previous experimental studies [22-23].

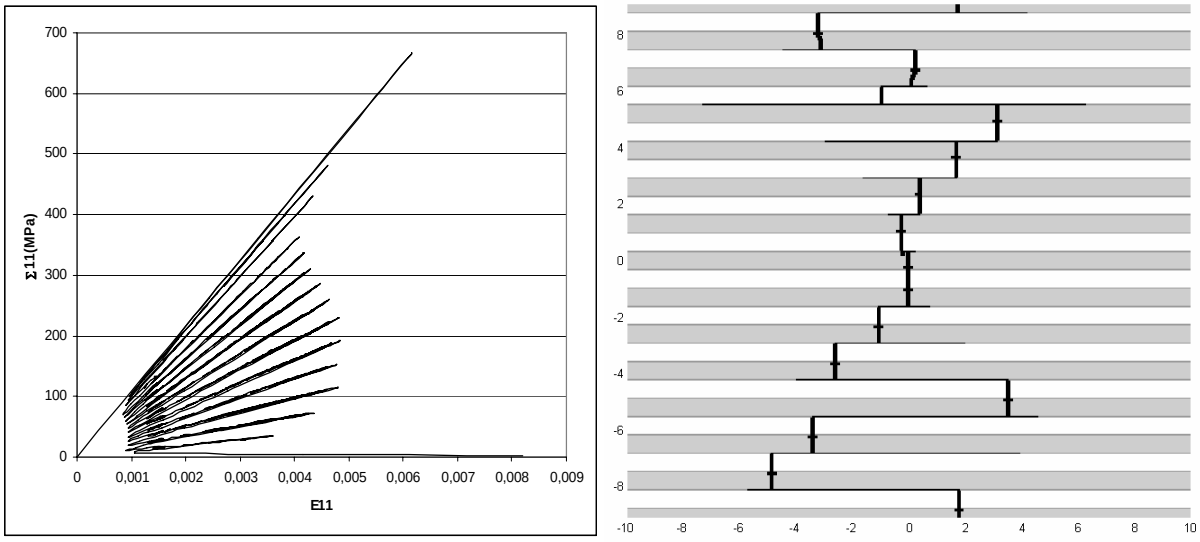

(c) (d)

Figure 3: Global response (a) and fracture patterns at the beginning (b), the middle (c) and the end (d) of the failure process of the basic cell under uniaxial tension

5: Discussions and concluding remarks

In this work, we have established a non-local fracture model and resolved it by using the Fast Fourier Transforms (FFT). The maximal stress criterion was adapted by means of the non-local concept in order to describe the fracture in brittle and quasi-brittle materials. The non-local model enables the predicted damage to be independent of the grid size. Moreover, the proposed model is equivalent to the Griffith-Irwin criterion when a macro-crack is formed. Consequently, the proposed fracture model is capable to predict crack initiation as well as crack growth. Comparisons with analytical results on pure mode-I cracks show that the proposed approach is highly efficient and accurate.

Through the examples above-presented, we can confirm that the proposed non-local crack growth models are highly accurate and efficient for the prediction of crack onset and crack propagation. Fracture in complicated microstructures can easily be simulated. Another notable advantage of the present method is its capacity to evaluate multiple crack growth as it doesn't require the calculation of the energy release rate at each crack tip. The theoretical concept of the proposed non-local fracture criterion is clear and simple. The numerical model is robust, easy to apply to different engineering structures subjected to thermal shock.

References

[1] McClintock, F. A., 1958. Ductile Fracture Instability in Shear. J. Appl. Mech., 10, 582-588
[2] Irwin G, (1968), Linear fracture mechanics, fracture transition and fracture control, Eng. Fract. Mech., 1:241-257
[3] Ritchie, R., Knott, J., and Rice, J., 1973. On the Relation between Critical Tensile Stress and Fracture Toughness in Mild Steel. J. Mech. Phys. Solids, 21, 395-410
[4] Seweryn, A., Lukaszewicz, A., 2002. Verification of Brittle Fracture Criteria for Elements with V-shaped Notches. Eng. Fract. Mech., 69, 1487-1510
[5] Leguillon, D., 2002. Strength or Toughness? A Criterion for Crack Onset at a Notch, Eur. J. Mech. A/Solids, 21, 61-72
[6] Barenblatt, G., 1959. The Formation of Equilibrium Cracks During Brittle Fracture, J. Appl. Math. Mech., 23, 434-444.
[7] Dugdale, D., 1960. Yielding of Steel Sheets Containing Slits. J. Mech. Phys. Solids, 8, 100–104.
[8] Xu, X. P., and Needleman, A., 1994. Numerical Simulation of Fast Crack Growth in Brittle Solids. J. Mech. Phy. Solids, 42, pp. 1397-1434
[9] Camacho, G.T., and Ortiz M., 1996. Computational Modelling of Impact Damage in Brittle Materials, Int. J. Solids Struct., 33, 2899–938.
[10] Mohammed, I., and Liechti, K.M., 2000. Cohesive Zone Modelling of Crack Nucleation at Bimaterial Corners. J. Mech. Phys. Solids, 48, 735–64.
[11] Pijaudier-Cabot, G., Bazant, Z.P., 1987. Nonlocal damage theory. J. of Engng. Mechanics, ASCE, 113, 1512-1533.
[12] Peerlings, R., de Borst, R., Brekelmans, W., De Vree, J., Spee, I., 1996. Some observations on localisation in non-local and gradient damage models. Eur. J. Mech. A/Solid, 15(6), 937-953
[13] Frémond, M., Nedjar, B., 1996. Damage, gradient of damage and principle of virtual power. Int. J. Solids Struct. 33, 1083-1103
[14] Francfort, G., Marigo, J-J., 1998. Revisiting brittle fracture as an energy minimization problem, J. Mech. Phys. Solids, 46, 1319-1342.
[15] Bourdin, B., Francfort, G., Marigo, J-J., 2000. Numerical experiments in revisited brittle fracture, J. Mech. Phys. Solids, 48, 797-826.
[16] Williams ML, (1961), The bending stress distribution at the base of a stationary crack. J. of Appl. Mech., 28:78–82
[17] Moulinec H, Suquet P (1998), A numerical method for computing the overall response of nonlinear composites with complex microstructure. Comput. Methods Appl. Mech. Engrg.; 157:69–94

[18] Li Jia, Tian Xiao Xiao, Abdelmoula Radhi, A damage model for crack prediction in brittle and quasi-brittle materials solved by the FFT method, International Journal of Fracture, 2012, Vol 173:135–146
[19] Ostoja-Starzewski M, Sheng PY, Alzebdeh K, (1996), Spring network models in elasticity and fracture of composites and polycrystals. Comput. Mater Sci., 7: 82–93
[20] Karihaloo BL, Shao PF, Xiao QZ, (2003), Lattice modelling of the failure of particle composites. Engng. Fract. Mech., 70-2385–2406
[21] Lilliu G, van Mier JGM., (2003), 3D lattice type fracture model for concrete, Engng. Fract. Mech., 70:927–941
[22] Raynaud C. Céramique lamellaires monolithiques en carbure de silicium, PhD Thesis, Ecole Nationale des Mines de St Etienne and Institut National Polytechnique de Grenoble, 2002.
[23] Tariolle S. Carbure de bore monolithique poreux et composites laminaires. PhD Thesis, Ecole Nationale des Mines de St Etienne and Institut National Polytechnique de Grenoble, 2003.